

Performance Analysis of Long-Cycle Small PWR Core with Coating Type Burnable Absorber and Different Reflectors

Woo Jin Lee, Sung Hyun Cho and Ser Gi Hong*

Departments of Nuclear Engineering, Hanyang University, 222, Wangsimni-ro, Seongdong-gu, Seoul, 04761, Republic of Korea

*Corresponding author: hongsergi@hanyang.ac.kr

1. Introduction

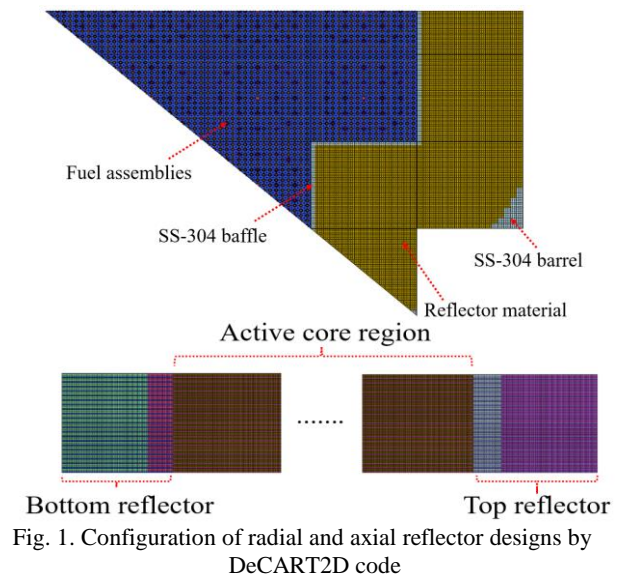
A small modular reactor (SMR) has recently attracted attention in many countries as a potential solution to the problem of climate change and the safety of traditional large reactors. Different types of SMR such as NuScale (PWR) in the U.S. and HTR-PM (VHTR) in China are being developed, and Korea has also been developing PWR-based SMR such as SMART [1]. Most of the PWR-based SMRs use soluble boron for controlling long-term reactivity change over a cycle. However, use of soluble boron can cause many issues such as corrosion of the primary system, complexity of Chemical and Volume Control System (CVCS), and boron dilution accidents. On the other hand, boron free operation also has technical issues such as licensing issue related to General Design Criteria (GDC) 26 for redundancy of reactivity control system and requirement of innovative burnable absorbers. Another issue for PWR-based SMRs is to enhance the economic performance. From the core physics aspect, it can be achieved by extending core cycle length, which can reduce fuel cost and increase capacity factor.

Our previous study showed that Gadolinium (III) Nitride coating Burnable Absorber (GdN-CBA) is a good candidate for low boron or boron-free operation [2]. However, the previous work was done only in the fuel assembly level calculation. As the next step, the objective of this work is to design a long-cycle (> 4 EFPYs) PWR-based SMR core with low boron concentration (< 400 ppm) using GdN-CBA rods. The following strategies were used to achieve long-cycle low boron core: 1) Excess reactivity control with optimized coating thicknesses of GdN-CBA and 2) Achievement of long cycle with solid-based radial and axial reflectors along with axial zoning strategy.

2. Modeling and Reflector Designs.

The two-step procedure comprised of the fuel assembly (FA) depletion calculation and the core depletion calculation is used in this work. The fuel assembly depletion calculations were performed using DeCART2D code developed by the Korea Atomic Energy Research Institute (KAERI) to generate the homogenized group constants (HGC) for core nodal diffusion calculations [3]. Then, the core depletion calculations were performed by using the MASTER code which is a 3D core depletion code developed by

KAERI [4]. In particular, the reflector modeling was performed by octant core heterogeneous calculations with DeCART2D to accurately produce the homogenized two group reflector cross sections. Fig. 1 shows the radial reflector and axial reflector models. The 2D octant core model considers the radial reflector consisting of stainless steel 304 (SS304) baffle and a barrel. We considered several candidate materials for reflector. A simplified 2D core model was used for the axial reflectors in which the fuel assemblies are surrounded by axial reflector and they are arranged in 1D array. The simplified 2D core model for axial reflectors assumes normal UO_2 pellets with gap, cladding, and moderator in the active core region, while the top and bottom reflector regions consist of stainless steel 304 support structure and reflector materials, with moderator passing between them.



3. Design Analysis and Results

3.1 Fuel Assembly and Core Design

Fig. 2 shows the GdN-CBA rod design where GdN layer is coated on UO_2 fuel pellet. GdN-CBA has similar structure like IFBA, but it is coated by cutting the outside of the UO_2 pellet. GdN-CBA is a good candidate for burnable absorber material because it has high thermal neutron absorption cross-section, high melting point, and thermal conductivity and it has no helium gas emission differently from IFBA [2,5]. In our

previous work, it was shown that GdN-CBA can have smaller residual penalty on the cycle length reduction than the conventional gadolinia burnable absorber [2].

Table I summarizes the design parameters of the fuel assemblies. As shown in Table I, the pitch of fuel rods is considerably increased from 1.26 cm to 1.32 cm so as to increase reactivity and to make moderator temperature coefficient (MTC) less negative because low boron or boron-free operation core will have very strong negative MTC [6]. Actually, this approach is inspired by the KAIST's truly optimized PWR paper even if our dimensions are different from that [7]. After optimizing the P/D ratio, the effect of GdN-CBA coating thickness on reactivity variations was analyzed. From the analysis, it was observed that each coating thickness resulted in different points at which gadolinium is almost depleted and in the different reactivity change curves [6]. Based on these observations, we identified the coating thicknesses that exhibit the similar points at which minimum and maximum reactivity occur. By combining these coating thicknesses, we successfully achieved fuel assembly designs giving low and relatively flat reactivity changes.

As a result, the parameters of the FAs finally designed for low boron concentration core design are shown in Table II. The selected 17x17 FAs have different combinations of coating thicknesses and numbers of GdN-CBA. The pitch between FAs is 22.6278 cm which is increased from its original value of 21.5 cm, and the uranium enrichment is 4.95 wt% for all fuel rods to extend the cycle length. Fig. 3 shows an example of fuel assembly configuration (1/8) with GdN-CBAs.

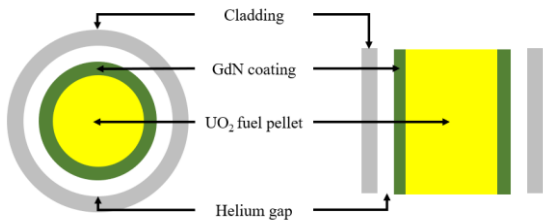


Fig. 1. Radial and axial configurations of GdN-CBA coated fuel pellet.

Table I: Design parameters of fuel assemblies

Design parameter of fuel assemblies	
Fuel rod array square	17x17
FA pitch	22.6278 cm
Fuel pin pitch	1.32 cm
Number of instrumental / guide tubes	25
Number of fuel rod	264
Fuel pellet density	10.220 g/cm ³
U-235 enrichment	4.95 wt. %
Fuel pellet radius	0.4096 cm
Fuel cladding inner radius	0.4178 cm
Fuel cladding outer radius	0.4750 cm
Cladding material	Zircaloy-4

Table II: Design parameters of fuel assemblies for low boron concentration core

Type	A0	A1	B1	C1	C2	D1
BA coating thickness (μm)	40 / 4 120 / 4 350 / 8 550 / 4 800 / 16	40 / 4 200 / 4 375 / 8 720 / 16	120 / 8 350 / 8 550 / 4 720 / 8	200 / 8 350 / 8 550 / 8	40 / 8 160 / 8 410 / 12	20 / 4 120 / 4 200 / 8
Number of BA in FA						
Total #	36	32	28	24	28	16

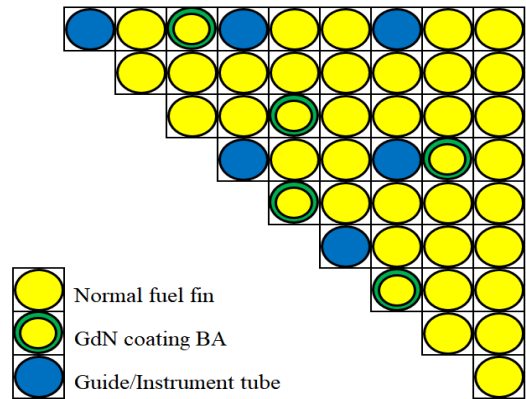


Fig. 3. Configuration of fuel assembly (1/8)

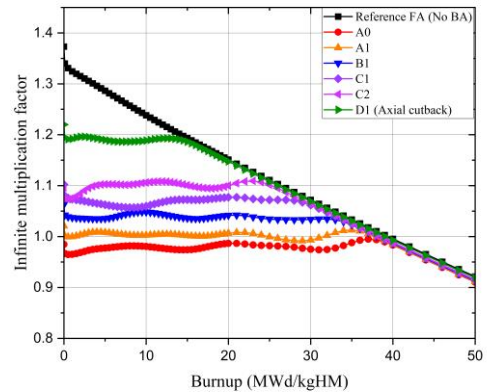


Fig. 4. Comparison of k_{inf} with respect to FAs

Fig. 4 compares the evolutions of k_{inf} of the selected fuel assemblies. Fig. 4 shows that the designed assemblies with various thickness combinations exhibit minimal fluctuations in k_{inf} . Table II and Fig. 4 show that increasing the number of BAs and using thicker coatings lead to an overall decrease in k_{inf} value, as expected. For example, The A0 assembly exhibiting the lowest overall k_{inf} value has 36 GdN-CBA rods and utilizes a maximum thickness of 800 μm. However, there are little residual reactivity penalties on cycle

length for all FAs regardless of thickness and number of GdN-CBA rods.

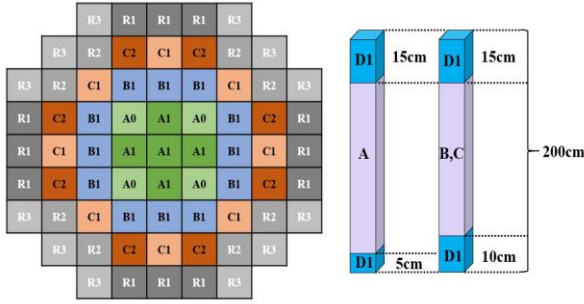


Fig. 5. Radial and axial configuration of core design

Fig. 5 shows the radial and axial configuration of our new core design for low boron operation. The core is loaded with A0, A1, B1, and C1, C2 fuel assemblies, which are surrounded by reflectors (i.e., R1, R2, and R3). In order to flatten radial power distribution, A-type assemblies having large number of BAs are loaded on the inner region of the core, while B and C type ones are loaded on the periphery of the core. Usually, a core having low critical boron concentration (CBC) results in a more negative MTC, skewing core's power distribution downward due to higher moderator density in lower region. To overcome it, a longer upper axial cutback of 15 cm was introduced in addition to a shorter lower axial one of 5 or 10cm, which also increases the cycle length. The D1 assembly having small number of BA rods was used both for lower and upper axial cutbacks.

Table III summarizes the design parameters and targets of the core design. The core generates 180MWth thermal power and is 200cm tall. It consists of 37 fuel assemblies. This core adopts one batch fuel management. We adopted a lower linear power density (84.2W/cm) and considered various solid-based reflectors to reduce neutron leakages in order to achieve long cycle length (> 4 EFPYs).

Table III: Design parameters and targets of core design

Parameters	Values
Full core power	180 MWth
Active core height	200 cm
Equivalent core diameter	158.3 cm
Average linear power density	84.2 W/cm
Fuel management scheme	One batch
Number of FAs in core	37
Maximum CBC over cycle	400 ppm
Minimum cycle length	4 EFPY (=1460 EFPD)
Maximum F_{xy} / F_{xyz}	2.0 / 2.5
AO range	-0.3 < AO < 0.3

3.2 Core Analysis Results with Different Reflectors

Our SMR core consists of 37 FAs, which accounts for approximately 20% of the FAs typically employed in existing commercial PWRs. Therefore, as the core size decreases, neutrons leakage from outside the core increases, which can significantly affect the cycle length. To address this issue, a more effective reflector is required, surpassing the water reflector commonly used in commercial PWR reactors. To extend the cycle length by reducing neutron leakage, solid-type reflector materials were employed as follows: 1) SS-304, 2) Zircaloy-4, 3) Zirconium Carbide (ZrC), 4) Graphite, and 5) Beryllium Oxide. These materials have small absorption cross-sections and large scattering cross-sections. First, the impact of the replacement of water radial reflector was analyzed. Then, we considered an axial reflector alongside the radial reflector to assess the influence of the axial reflector in the SMR core.

Fig. 6 compares the evolutions of CBC for the different radial reflector materials. From the analysis, it was shown that replacing the water reflector with SS304, Zircaloy-4, Zirconium carbide, Graphite, and Beryllium oxide led to increases in cycle length by 289.3, 308.7, 348.6, 402.9, and 441.2 EFPDs, respectively. On the other hand, the increases in cycle lengths are accompanied by increases in maximum critical boron concentration (CBC) by 214.59, 231.08, 265.39, 315.66, and 356.84 ppm, respectively. Also, it was observed that the reflector materials giving longer cycle lengths showed more decreases in the 2D power peaking factor (F_{xx}) as shown Fig. 7. This radial power flattening is resulted from the effective thermal neutron scattering by the solid reflector materials. Table IV presents the radial reflector material densities, and the effects of the considered reflectors on the selected main core performance parameters. All densities were initially assumed to be at their theoretical values before irradiation.

All solid-type reflector materials achieve the negative MTC both at BOC and EOC under Hot Zero Power (HZP) and Hot Full Power (HFP) conditions. However, Beryllium Oxide does not meet some of the design criteria. While achieving the longest cycle length of 1616 EFPDs, CBC of the Beryllium Oxide reflector case exceeded the 400ppm design criterion. Also, Beryllium Oxide is known to be toxic and expensive material. It is also noted that the cores having the considered solid reflectors have small power peaking factors.

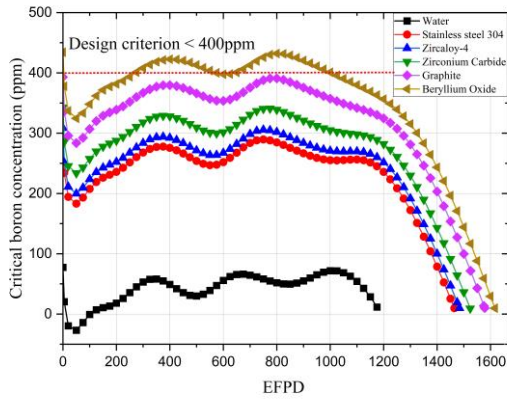


Fig. 6. Comparison of CBC with respect to different radial reflector materials

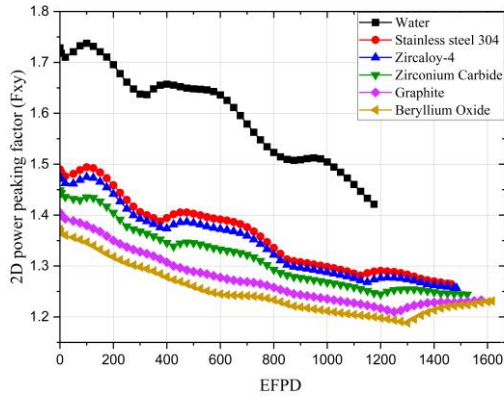


Fig. 7. Comparison of 2D power peaking factor with respect to different radial reflector materials

Table IV: Summary of radial reflector performances

Reflector	Water	SS304	Zircaloy4	Zirconium Carbide	Graphite	Beryllium Oxide	
Density (g/cm ³)	0.719	7.9	6.55	6.73	2.25	3.01	
Cycle length (EFPD)	1175	1464	1483	1523	1577	1616	
Burn up (MWd/kgHM)	23.2	28.9	29.3	30.0	31.1	31.9	
Maximum CBC (ppm)	77.43	292.02	308.51	342.82	393.09	434.27	
Maximum F _{xy}	1.7377	1.4941	1.4763	1.4490	1.4048	1.3719	
Maximum F _{xyz}	2.2603	1.9323	1.9139	1.8775	1.8190	1.7754	
Maximum Axial Offset in absolute value	0.0492	0.0274	0.0257	0.0257	0.0157	0.0167	
MTC (pcm/°C)	HFP (BOC / EOC)	-58.4 / -60.75	-47.58 / -58.29	-47.85 / -58.24	-45.45 / -57.51	-42.6 / -55.89	-40.35 / -54.77
	HZP (BOC / EOC)	-39.03 / -36.68	-31.89 / -36.84	-31.44 / -36.85	-30.23 / -36.61	-28.26 / -35.77	-26.64 / -35.18

An axial neutron leakage is also significant in the SMR core. Although the performance of most radial solid reflectors already met the long-cycle requirements, we also applied solid-type axial reflectors together to achieve a slightly longer-cycle length while satisfying

the design criteria. The details of design are illustrated in Section 2 with Fig. 1. ZrC, which exhibited a good reflector effect, was applied as both the axial and radial reflector material.

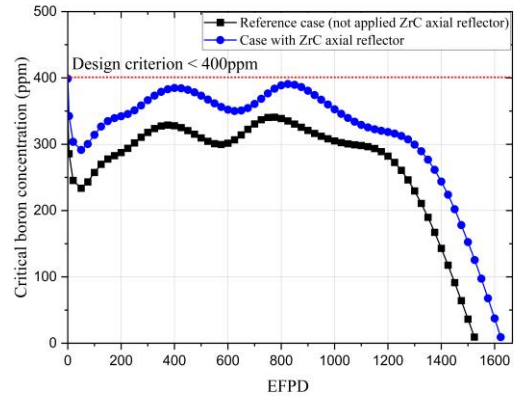


Fig. 8. Comparison of CBC with respect to axial reflector materials: ZrC vs. Non-ZrC

Fig. 8 compares the evolution of CBC for the core having ZrC axial and radial reflectors, and the core having only ZrC radial reflector. When ZrC was used as the axial reflector, the cycle length increased by 98 EFPD, giving a total cycle length of 1622EFPD, and a maximum CBC of 398 ppm. This analysis shows the ZrC solid-type axial reflector gives the benefits in terms of the extended cycle length by effectively reducing axial neutron leakage. The 3D power peaking factor (F_{xyz}) is also decreased overall due to reduction of axial neutron leakages as shown Fig. 9. Fig. 10 compares the evolution of axial offset (AO) in ARO (All Rods out) states. Before the application of the ZrC axial reflector, the axial power distribution was slightly downward skewing at both BOC and MOC. However, the application of the ZrC axial reflector caused upward skewing through BOC to MOC, resulting in a maximum axial offset of 0.0422 in absolute values, satisfying the design criteria of AO.

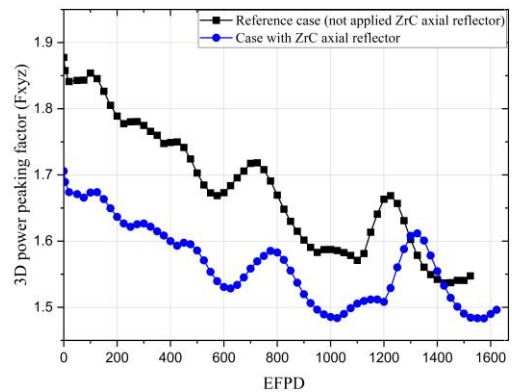


Fig. 9. Comparison of 3D power peaking factor with respect to axial reflector materials: ZrC vs. Non-ZrC

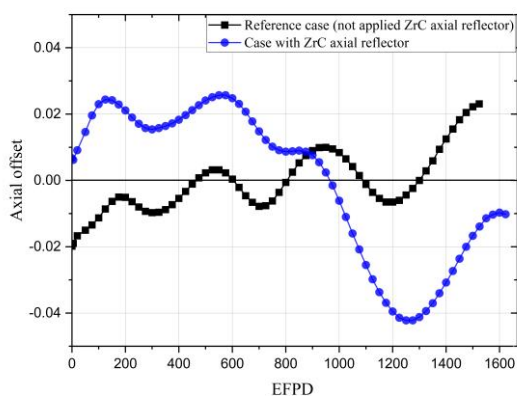


Fig. 10. Comparison of axial offset with respect to axial reflector materials in ARO states: ZrC vs. Non-ZrC

4. Conclusions

In this work, 180 MWt long-cycle PWR-based SMR cores were designed using the fuel assemblies employing optimized fuel assemblies using GdN-CBA rods. In particular, the fuel assemblies were designed by searching the desirable combinations of the GdN coating thickness and number of GdN-CBA rods so as to achieve flat change of reactivity. As the result, six fuel assemblies were finally selected and they were used in the core design. The effects of the solid radial and axial reflectors on the core performances were also analyzed by considering several solid reflector materials for the SMR core. For this purpose, the two-group homogenized reflector cross sections were generated through heterogeneous 2D octant core transport calculations with DeCART2D. Also, the axial cutbacks are considered to make the axial power distribution flatter.

From the analysis, it was shown that 1) the GdN-CBA rods can be effectively used to achieve relatively flat reactivity change, 2) the solid reflectors are very effective to increase cycle length (e.g., uses of ZrC and SS304 radial reflectors increased cycle length by 348 and 289 EFPDs, respectively), and 3) the use of ZrC axial reflector to the SMR core having ZrC radial reflectors led to an additional cycle length increase by 98 EFPDs.

In conclusion, it was possible to a long-cycle PWR-based SMR core with ZrC solid reflectors which has 4.45 EFPYs cycle length and 398ppm maximum CBC, and satisfies all the other design criteria.

REFERENCES

- [1] Subki, M. Hadid. "Update on SMR technology status and IAEA programme on common technology and issues for SMRs." *INPRO Dialogue Forum on NE Innovations: CUC for SMR*. 2011.
- [2] S.H. Cho, S.G. Hong, "A Novel Burnable Absorber for Small Modular Reactors: Gadolinium (III) Nitride Coating",

Transactions of the Korean Nuclear Society Spring Meeting Jeju, Korea, May 18-19, 2023

[3] J. Y. Cho et al., "DeCART2D v1.0 User's Manual", KAERI/TR-5116/2013.

[4] J. Y. Cho et al., "MASTER v4.0 User's Manual", KAERI/UM-41/2016.

[5] Glen A. Slack and Sandra B. Schujman, "Deep-eutectic melt growth of nitride crystals", U.S. patent 8 088 220 B2, Jan. 3, 2012.

[6] S.H. Cho, W.J. Lee and S.G. Hong, "An Optimization Study of Fuel Assembly Designs with GdN-CBA Rods for Boron-Free Operation", *Transactions of the Korean Nuclear Society Autumn Meeting* Gyeongju, Korea, October 26-27, 2023.

[7] Nguyen, Xuan Ha, Seongdong Jang, and Yonghee Kim. "Truly-optimized PWR lattice for innovative soluble-boron-free small modular reactor." *Scientific reports* 11.1, 12891, 2021.